ROYAL SOCIETY OF CHEMISTRY

PERSPECTIVE

Check for updates

Unconventional aspects in metal-embedded laser-induced graphene

Arie Borenstein [ID] *[a] and Richard B. Kaner [ID] [b]

Laser-induced graphene (LIG) has gained significant attention, with over 170 publications in 2023 alone. This surge in popularity is due to the unique advantages LIG offers over traditional thermal methods, such as fast, solvent-free, scalable production and its ability to scribe intricate patterns on various substrates, including heat-sensitive materials like plastics. In recent developments, metal-embedded LIG (M-LIG) has expanded the potential applications of LIG, particularly in energy storage, microelectronics, and sensing. However, the complexity of the laser-induced reactions, especially those involving metal ions, has limited a thorough understanding of these processes. This perspective highlights the challenges of predicting the final oxidation states of metal nanoparticles formed during laser processing. Based on a survey of over 20 studies, we discuss the influence of reduction potential and other environmental factors, such as carbon precursors, on metal ion reduction. While reduction potential strongly correlates with product formation, inconsistencies across experiments suggest additional factors, such as reaction kinetics, diffusion rates, and crystallization, play critical roles. Future research should focus on controlling oxidation states and particle size, the formation of bimetallic structures, and atomically-dispersed metals in graphene, to better harness the full potential of M-LIG materials.

Introduction

Since our pioneering publication in 2012,[1] the number of published studies on laser-induced graphene has experienced a steep and continuous rise, exceeding 170 annual publications in 2023. The rapid ascending popularity of this method can be attributed to the distinct benefits it holds compared to traditional thermal techniques, mainly (1) simple processing in terms of fast production, solvent and waste-free sustainability, cost-effectiveness, safety, and more; (2) patterning or scribing any desired shape; (3) areal scaling limited only by the size and wavelength of the laser. This property is of particular importance for microelectronic applications. (4) Direct coating on diverse substrates, including thermal-sensitive materials, *e.g.*, plastics; and (5) the fast laser-induced reaction can result in chemically unique and even nontrivial morphologies and phases. Interestingly, while being exposed to oxygen, the carbon precursors do not actually burn, but instead undergo extreme thermal carbonization processes. Combining all these advantageous features, it becomes clear why laser carbonization has been implemented in diverse applications such as energy storage, microelectronics, communications, sensing, bioprotection, and more.

Later, metal ions were incorporated into carbon precursors to produce metal-embedded laser-induced graphene (M-LIG). Introducing metals widens the possible functionalities and potential applications. Usually, metal salts or complexes are mixed with the carbonaceous precursors, and the irradiated laser simultaneously converts both the carbon and metals. While the carbon tends to be reduced into different forms of graphitic carbon, the final forms of the accompanying metals are hard to anticipate. Moreover, much research has focused on understanding the thermochemical reactions involving carbon reduction into graphene. However, understanding of the parallel reaction with metal ions has been much less studied. Out of the 175 laser-induced graphene papers published in 2023, only 18 are associated with M-LIG. This perspective aims to highlight the complexity of metals involved in laser processing and to discuss possible relevant parameters that affect the laser-induced reactions resulting in the formation of metal-based nanoparticles. It is important to note that some studies use short laser wavelengths that might induce photochemical reactions. This perspective, however, is focused on long wavelength lasers (such as CO_2) and on the thermal processes that are induced in the irradiated films. A detailed study on laser-induced photochemical reactions deserves a separate perspective.

Complexity challenges

The complexity of measuring and understanding the mechanism(s) of laser-processed carbon arises from the high

[a]Department of Chemical Sciences, Ariel University, Ariel, Israel. E-mail: arieb@ariel.ac.il

[b]Department of Chemistry & Biochemistry, Department of Materials Science & Engineering, California NanoSystems Institute, University of California, Los Angeles, Los Angeles, CA 90095, USA. E-mail: kaner@chem.ucla.edu

Table 1 Different metals co-participating in laser processing along with the lasering parameters and selected properties of the precursors and final laser products

Metal	Final phase	Oxidation state	Red. potential[a]	Metal precursor	Laser parameters	Surrounding	Ref. #
Mn	MnO_2, Mn_3O_4	+2, +3, +4	−1.17	$Mn(CH_3COO)_2$	2.2 W, 100 mm s^{-1}	GO	5
	MnO_2	+2, +3, +4	−1.17	Mn(II) phthalocyanine	5 to 10 W	Biomass gelatin	6
	Mn_3O_4						
V	VO_x	+3, +5	−1.13	V_5S_8		Pluronic F127	7
Mo	MoO_2	+4	−0.913	$(NH_4)_2MoO_4$	2 to 3.5 W, 50 mm s^{-1}	Carbon cloth	8
Zn	ZnO	+2	−0.76	$Zn(C_2H_3O_2)_2$	5 W, 10 mm s^{-1}	CND	Our work
	ZnO	+2	−0.76	Zn metal powder	15–27 W, 100–350 mm s^{-1}	PI	9
Fe	Fe_3O_4	2.66	−0.44	$Fe(acac)_3$	5 W	GO	10
Co	Co_3O_4	2.66 (+2/+3)	−0.28	$Co(NO_3)_2$	2.5 W	LIG (GO)[b]	11
	Co_3O_4	2.66 (+2/+3)	−0.28	$Co(OAc)_2$	1.5 W	PI	12
	Co_3O_4	2.66 (+2/+3)	−0.28	$Co(NO)_3·6H_2O$	2 W	GO	13
	Co_3O_4	2.66 (+2/+3), +2	−0.28	$Co(OAc)_2·4H_2O$	5.1 W, 10 mm s^{-1}	PFA	14
Ni	NiO, Ni	+2, 0	−0.257	$Ni(acac)_2$	2W	PI	15
	NiO, Ni	+2, 0	−0.257		2.5 W, 10 mm s^{-1}	GO	Our work
Sn	SnO	+2	−0.136	$SnCl_2·2H_2O$	355 nm laser, 10 W	GO	16
C	$CO_2^+(g) + 2H^+ + 2e^- \rightleftharpoons CO(g) + H_2O(l)$, $E = -0.106$						
Cu	Cu	0	0.319	HKUST-1	Pulse laser, 3.5–7.5 W, 75 mm^{-1}	HKUST-1	17
	Cu	0	0.319	Cu(acac)	5 W, 10 mm s^{-1}	CND	Our work
	Cu	+1	0.319	HUST-1	6.25 W, 80 mm s^{-1}	HKUST-1	Our work
	Cu_2O, CuO	+1, +2	0.52	Cu(acac)	1.5 W, 20 mm s^{-1}	GO	13
Ag	Ag	0	0.799	$AgNO_3$(I)	2.20–3.85 W, 1 to 3 cm s^{-1}	PI	18
	Ag	0	0.799	CH_3OOAg	Not specified	GO	19
Pd	Pd	0	0.915	$PdCl_2$		Chitosan, PI	20
	Pd	0	0.915	$Pd(NO_3)_2·xH_2O$		GO	Our work
Pt	Pt	0	1.2	$Pt(acac)_2$	5.1 W, 10 mm s^{-1}	PFA	14
	Pt	0	1.2	H_2PtCl_6	2.20–3.85 W, 1 to 3 cm s^{-1}	PI	16
Au	0	0	1.83	$HAuCl_4·3H_2O$(III)	2.20–3.85 W, 1 to 3 cm s^{-1}	PI	18

[a] Potentials vs. SHE, $2H^+(aq.) + 2e^- \rightleftharpoons H_2(g)$. [b] Second laser processing after metal solution deposited on already lasered rGO.

heterogeneity of the reaction(s). First, the photo-irradiation induces uneven heating throughout the irradiated sample. As demonstrated by Strauss et al., the upper area of the carbonaceous film is subjected to significantly stronger heating than its lower parts.[2] This directly results in different chemical and morphological compositions along the thickness of the film. Likewise, the lasered film is uneven laterally as well since areas that were directly hit by the laser beam demonstrate full graphitization, while the peripheral regions undergo only partial conversion with a gradient. Of course, metals introduced into the precursor film face similar heterogeneity, hence doubling the complexity of the reaction(s).

The main open questions we wish to address in this perspective regard the oxidation states of the laser-resulting metal-based nanoparticles. In other words, can we anticipate whether the metal ions will form oxide nanoparticles or will be reduced into metallic nanoparticles? By now, there is a lack of publications that have addressed these questions. Tour et al. explicitly addressed this question and suggested that CO serves as a reducing agent for both carbon and metals.[3] According to this theory, when CO is eliminated by the laser, carbon disproportionates and is oxidized into CO_2 while reducing oxidized carbon into graphene. Similarly, it can also reduce the metal cations into metals. Following this explanation, the authors suggest that the chemical composition of the carbon precursors (lignin or cellulose, in that case) can determine the post-laser oxidation state of the metal. However, while this explanation appears to be reasonable, other parameters must still be considered. First, CO was reported to be a byproduct of laser scribing of polyimides as well, and yet, metals incorporated with polyimides were reported to form oxides, rather than reduced metals.[4] Additionally, to achieve metal reduction, the lasering in the mentioned study was conducted under an argon atmosphere. Not only is the simplicity of the process lessened, but the cellulose itself consists of 23.8% oxygen, questioning the oxygen-free conditions of the reaction.

For a more comprehensive understanding, we would like to highlight other complementary parameters. To detect the parameters that dominantly influence the laser-induced metal reaction, we analyzed data collected from over 20 publications combined with new experimental observations accumulated in our labs. The analyzed data are summarized in Table 1. Notice that studies using already prepared metal or metal oxide nanoparticles mixed with carbon and subjected to lasering were not taken into account in this survey since the oxidation state of the metal was determined prior to the laser reaction.
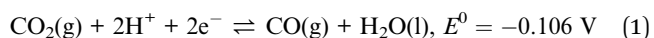
Reduction potential dependent

The first finding from the survey is the immense dependence on reduction potential. For instance, while zinc formed zinc oxide (ZnO) in all publications, regardless of the carbon precursors or

laser conditions, palladium consistently yielded metallic phases. On the other hand, the structures formed by iron are more complex, demonstrating partial oxidation and generating a mixture of +2 and +3 particles in the same sample (Fe_2O_3, Fe_3O_4). At the same time, manganese displays an even broader spectrum of oxidation states ranging from +2 to +4 (MnO_2, Mn_3O_4). Moreover, different metals behave differently under the same conditions. This was demonstrated by Pope *et al.*, who reported a Pt–Co bimetallic laser product where the platinum was fully reduced (Pt^0), while the cobalt with one laser treatment mainly resulted in $Co^{2.6+}$.[14]

Generally, when a redox reaction occurs, the reduction potentials of the two participating compounds should be compared. Notably, CO_2 is reduced into CO in the following reaction, with a reduction potential of -0.106 V *vs.* SHE.

$$CO_2(g) + 2H^+ + 2e^- \rightleftharpoons CO(g) + H_2O(l), \; E^0 = -0.106 \text{ V} \quad (1)$$

Thermodynamically, all substances with higher reduction potentials are susceptible to being reduced by CO, and metal ions with lower reduction potentials are anticipated to remain oxidized. Fig. 1 clearly shows the strong correlation between the oxidation state of the M-LIG products with the reduction potential of that metal. The *R*-value of the linear trending line is 0.774. Indeed, most of the elements with lower reduction potentials were not reduced and were sometimes oxidized. All elements with higher reduction potentials were reduced, with the exception of copper, which, in some studies, retained its +2 oxidation state. Here, we note the potential of the reported oxidation state of the metallic precursor for the reduction reaction: $M^{x+} + xe^- \rightarrow M(s)$, where M is the metallic element, x is the charge of the cation, and M(s) is the metallic form of the element.

Effect of environmental composition

Yet, while reduction potential is a significant factor, this seems to oversimplify and only partially dictates the outcome, as evidenced by discrepancies in reduction outcomes among different experiments (and conditions) of the same metals. Indeed, evidence is found for the role of the surrounding chemical environment, namely, the carbon precursor. For example, Cu-LIG produced CuO nanoparticles when mixed with a graphene-oxide (GO) film, while forming metallic Cu^0 particles when mixed with carbon nanodots (CND) under the same conditions. In this case, not only do carbon nanodots not contain oxygen, but the nitrogen-doped CNDs may also contribute to the reductive environment. The electron-rich N atoms are oxidized to form molecular nitrogen (N_2), while reducing the metals in the process. Interestingly, when the metal organic framework (MOF) HKUST-1 was lasered, the copper +2 ions, coordinatively bonded to oxygen, formed two phases of copper oxides (CuO and Cu_2O, Fig. 2a).

Kinetics, diffusion, and crystallography

Other aspects must be considered. First, the kinetics of the oxidation and reduction reactions are likely to play a critical role. One kinetic aspect directly responsible for a major process in the creation of nanoparticles is diffusion rates. The metal ions are initially atomically dispersed in the carbon precursors. Then, upon laser treatment, they have to diffuse, nucleate, and grow in order to form nanoparticles. Like every diffusion-controlled reaction, the final size of the particles depends on the concentration of the metal ions. This phenomenon is reported in many publications, and was documented in our labs for copper nanoparticles (Fig. 2b).[21] Furthermore, crystallization may be
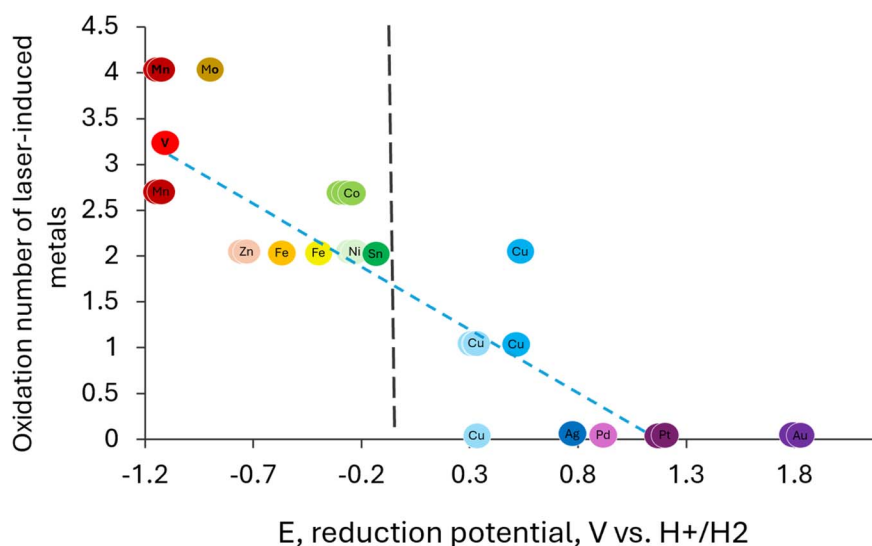

Fig. 1 The oxidation state of laser-induced metals *vs.* the reduction potential, referring to $M^{x+} + xe^- \rightarrow M(s)$. Each color represents a different element. The black line represents the potential of carbon monoxide oxidation. The dashed blue line represents the linear trend. The data and references are presented in Table 1.
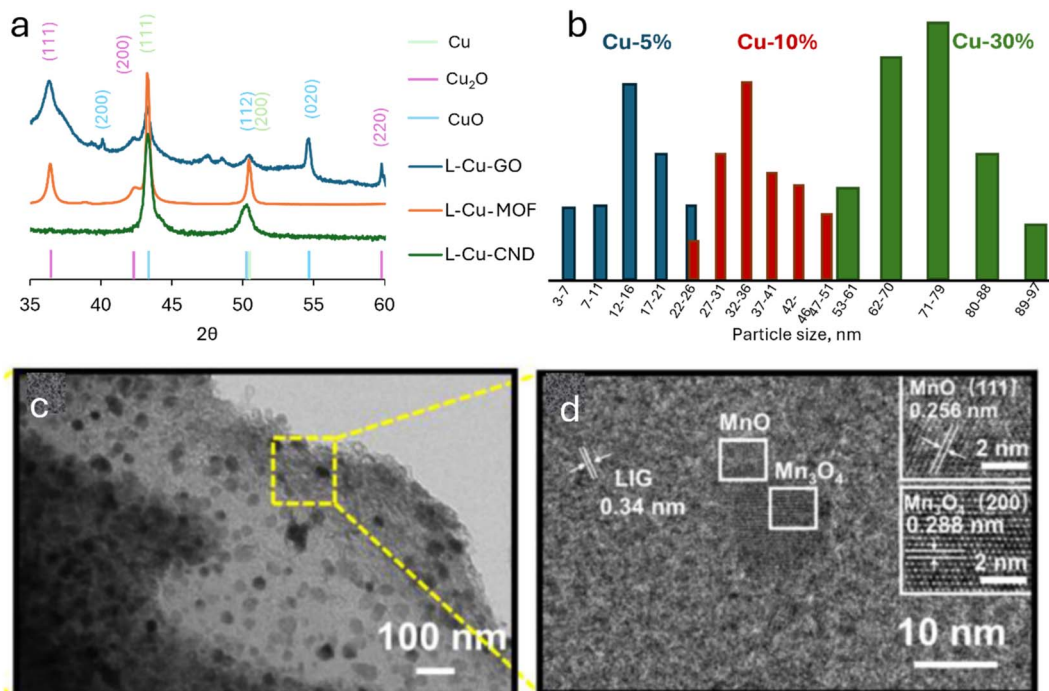
Fig. 2 M–LIG reveals unconventional phenomena. (a) XRD spectra exhibit different copper phases formed from Cu^{2+} ions with varying carbon precursors. (b) Particle size distributions formed from three concentrations of Cu^{2+} ions lasered under the same conductions. (c) TEM image, (d) HRTEM image and of MnO_x@LIG showcasing two manganese-oxide phases in the same particle (taken from ref. 5).

a relatively slow reaction compared to the reduction reaction. Therefore due to the rapid reaction, the particles may not have enough time to fully crystallize. Laser power may also affect the M-LIG products according to phase diagrams, where the more oxidated phases are usually more stable at lower temperatures.

As mentioned above, laser-induced thermal reactions occur in milliseconds. Considering the high thermal conductivity of carbon, heat diffuses through the materials rapidly and accelerates both heating up and cooling down. This affects not only the carbon conversion, but also the metal ions. Often in these rapid reactions, the materials don't reach a steady-state, and therefore, the preferred pathway may be the faster reaction rather than the more stable one. This leads to the formation of meta-stable phases. The observation of multi-phase metals in a single particle demonstrates this phenomenon. For example, Huang et al. captured an HR-TEM of a particle comprising both MnO and Mn_3O_4 (Fig. 2c and d).[5]

Conclusions and future perspectives

In conclusion, in this perspective, we have highlighted the reduction potential dependence on the oxidation state of M-LIG. We also suggest other tunable factors affecting the phase, size, and crystallinity of the final laser products. Yet, the current understanding of laser processing of metal-carbon composites remains limited, with numerous questions in need of answers. More research is required in order to better understand the rapid reactions taking place during laser irradiation. Key areas for future exploration include the control of oxidation states and phases through tuning of laser parameters, successfully

governing the formation of bimetallic particles including core–shell and gradient concentrations, laser fabrication of atomically-dispersed metals in graphitic matrices, and the feasibility of forming carbon-free metallic continuous thin films *via* laser processing. A direct real-time observation of the chemical processes involved in laser-induced conversion would certainly provide valuable insights. However, due to the rapid nature of the reaction, this remains experimentally challenging. Another possible method to track the reaction pathways is by isotopic labeling of the precursors and identifying the chemical changes by NMR. Addressing these questions through a combination of experimental and theoretical studies will not only enhance our understanding, but also pave the way for more precise control over the final products and the design of desired materials.

Data availability

No primary research results, software or code have been included and no new data were generated or analysed as part of this review.

Author contributions

Arie Borenstein: conceptualization and idea development, literature review, data analysis, writing, Richard B. Kaner: idea development, writing, reviewing, editing.

Conflicts of interest

There are no conflicts to declare.

Acknowledgements

References

1 M. F. El-Kady, V. Strong, S. Dubin and R. B. Kaner, Laser Scribing of High-Performance and Flexible Graphene-Based Electrochemical Capacitors, *Science*, 2012, **335**, 1326–1330, DOI: **10.1126/science.1216744**.

2 H. Wang, C. O. Ogolla, G. Panchal, M. Hepp, S. Delacroix, D. Cruz, D. Kojda, J. Ciston, C. Ophus, A. Knop-Gericke, K. Habicht, B. Butz and V. Strauss, Flexible CO_2 Sensor Architecture with Selective Nitrogen Functionalities by One-Step Laser-Induced Conversion of Versatile Organic Ink, *Adv. Funct. Mater.*, 2022, **32**(51), 2207406, DOI: **10.1002/adfm.202207406**.

3 X. Han, R. Ye, Y. Chyan, T. Wang, C. Zhang, L. Shi, T. Zhang, Y. Zhao and J. M. Tour, Laser-Induced Graphene from Wood Impregnated with Metal Salts and Use in Electrocatalysis, *ACS Appl. Nano Mater.*, 2018, **1**(9), 5053–5061, DOI: **10.1021/acsanm.8b01163**.

4 M. Inagaki, N. Ohta and Y. Hishiyama, Aromatic Polyimides as Carbon Precursors, *Carbon*, 2013, 1–21, DOI: **10.1016/j.carbon.2013.05.035**.

5 H. Xiao, Y. Li, R. Chen, T. Xie, P. Xu, H. Zhu, J. He, W. Zheng and S. Huang, Integrative Design of Laser-Induced Graphene Array with Lithiophilic MnO_x Nanoparticles Enables Superior Lithium Metal Batteries, *eScience*, 2023, **3**(5), 100134, DOI: **10.1016/j.esci.2023.100134**.

6 C. Zhou, K. Zhang, M. Hong, Y. Yang, N. Hu, Y. Su, L. Zhang and Y. Zhang, Laser-Induced MnO/Mn_3O_4/N-Doped-Graphene Hybrid as Binder-Free Anodes for Lithium Ion Batteries, *Chem. Eng. J.*, 2020, **385**, 123720, DOI: **10.1016/j.cej.2019.123720**.

7 L. Yang, J. Yan, C. Meng, A. Dutta, X. Chen, Y. Xue, G. Niu, Y. Wang, S. Du, P. Zhou, C. Zhang, S. Guo and H. Cheng, Vanadium Oxide-Doped Laser-Induced Graphene Multi-Parameter Sensor to Decouple Soil Nitrogen Loss and Temperature, *Adv. Mater.*, 2023, **35**(14), 2210322, DOI: **10.1002/adma.202210322**.

8 N. Lin, H. Chen, W. Wang and L. Lu, Laser-Induced Graphene/MoO_2 Core-Shell Electrodes on Carbon Cloth for Integrated, High-Voltage, and In-Planar Microsupercapacitors, *Adv. Mater. Technol.*, 2021, **6**(5), 2000991, DOI: **10.1002/admt.202000991**.

9 J. Rodrigues, J. Zanoni, G. Gaspar, A. J. S. Fernandes, A. F. Carvalho, N. F. Santos, T. Monteiro and F. M. Costa, ZnO Decorated Laser-Induced Graphene Produced by Direct Laser Scribing, *Nanoscale Adv.*, 2019, **1**(8), 3252–3268, DOI: **10.1039/c8na00391b**.

10 K. Sathiyan, A. Lal and A. Borenstein, Laser Processed Magnetite Nanoparticles Embedded on RGO Composites for Efficient Electrocatalytic Oxygen Evolution Reaction, *Adv. Sustainable Syst.*, 2022, **6**(7), 2200076, DOI: **10.1002/adsu.202200076**.

11 X. Ding, R. Liu, J. Zhao, J. Hu, J. Wu, C. Zhang and J. Lin, In Situ Formation of Co_3O_4 Nanocrystals Embedded in Laser-Induced Graphene Foam for High-Energy Flexible Micro-Supercapacitors, *Dalton Trans.*, 2022, **51**(7), 2846–2854, DOI: **10.1039/d1dt03848f**.

12 M. Ren, J. Zhang and J. M. Tour, Laser-Induced Graphene Synthesis of Co_3O_4 in Graphene for Oxygen Electrocatalysis and Metal-Air Batteries, *Carbon*, 2018, **139**, 880–887, DOI: **10.1016/j.carbon.2018.07.051**.

13 A. Lal, H. Porat, L. O. Hirsch, R. Cahan and A. Borenstein, Laser-Assisted Direct Coating of Graphene-Based Films on Plastic Substrates with Bactericidal Properties, *Appl. Surf. Sci.*, 2024, **643**, 158660, DOI: **10.1016/j.apsusc.2023.158660**.

14 T. R. Aldhafeeri, M. Uceda, A. Singh, M. Ozhukil Valappil, M. W. Fowler and M. A. Pope, Embedded Platinum-Cobalt Nanoalloys in Biomass-Derived Laser-Induced Graphene as Stable, Air-Breathing Cathodes for Zinc-Air Batteries, *ACS Appl. Nano Mater.*, 2023, **6**(10), 8302–8314, DOI: **10.1021/acsanm.3c00564**.

15 Z. Feng, Z. Geng, S. Pan, Y. Yin, X. Sun, X. Liu, L. Ge and F. Li, In Situ Patterning of Nickel/Sulfur-Codoped Laser-Induced Graphene Electrode for Selective Electrocatalytic Valorization of Glycerol, *Appl. Catal., B*, 2024, **353**, 124101, DOI: **10.1016/j.apcatb.2024.124101**.

16 A. E. M. Abd Elhamid, H. Shawkey, A. A. I. Khalil and I. M. Azzouz, Laser Writing of Graphene-tin Hybrid Composite-Based Supercapacitor for Battery-like Performance, *J. Energy Storage*, 2023, **73**(Part C), 109106, DOI: **10.1016/j.est.2023.109106**.

17 H. Jiang, L. Tong, H. Liu, J. Xu, S. Jin, C. Wang, X. Hu, L. Ye, H. Deng and G. J. Cheng, Graphene-Metal-Metastructure Monolith via Laser Shock-Induced Thermochemical Stitching of MOF Crystals, *Matter*, 2020, **2**(6), 1535–1549, DOI: **10.1016/j.matt.2020.03.003**.

18 Z. You, Q. Qiu, H. Chen, Y. Feng, X. Wang, Y. Wang and Y. Ying, Laser-Induced Noble Metal Nanoparticle-Graphene Composites Enabled Flexible Biosensor for Pathogen Detection, *Biosens. Bioelectron.*, 2020, **150**, 111896, DOI: **10.1016/j.bios.2019.111896**.

19 H. Shen, J. Liu, P. Pan, X. Yang, Z. Yang, P. Li, G. Liu, X. Zhang and J. Zhou, One-Step Synthesis of Nanosilver Embedding Laser-Induced Graphene for H_2O_2 Sensor, *Synth. Met.*, 2023, **293**, 117235, DOI: **10.1016/j.synthmet.2022.117235**.

20 A. Soleh, K. Saisahas, K. Promsuwan, J. Saichanapan, P. Thavarungkul, P. Kanatharana, L. Meng, W. C. Mak and W. Limbut, A Wireless Smartphone-Based "Tap-and-Detect" Formaldehyde Sensor with Disposable Nano-Palladium Grafted Laser-Induced Graphene (NanoPd@LIG) Electrodes, *Talanta*, 2023, **254**, 124169, DOI: **10.1016/j.talanta.2022.124169**.

21 H. Yao, L. Liu, S. Zhang, L. Wu, J. Tang, Y. Qiu, S. Huang, H. Wu and L. Fan, Metal-incorporated laser-induced graphene for high performance supercapacitors, *Electrochim. Acta*, 2023, **441**, 141719, DOI: **10.1016/j.electacta.2022.141719**.